Efficient evaluation of the nonstabilizerness in unitary and monitored quantum many-body systems

Angelo Russomanno,[1] Gianluca Passarelli,[1] Davide Rossini,[2] and Procolo Lucignano[1]

[1]*Dipartimento di Fisica "E. Pancini", Università di Napoli Federico II,*
Complesso di Monte S. Angelo, via Cinthia, I-80126 Napoli, Italy
[2]*Dipartimento di Fisica dell'Università di Pisa and INFN, Largo Pontecorvo 3, I-56127 Pisa, Italy*

We consider the quantum-state-diffusion dynamics of the staggered XXZ chain, also focusing on its noninteracting tight-binding limit, and of the SYK model. We describe the process through quantum trajectories and evaluate the nonstabilizerness (also known as "magic") along the trajectories, quantified through the stabilizer Rényi entropy (SRE). To do that we introduce a numerical method to evaluate SRE, more efficient than the brute-force one, based on the expansion of the state restricted to a subspace in the computational basis of the classical spin configurations. In the absence of measurements, we find that the SYK model is the only one where the time-averaged SRE saturates the fully-random state bound and has a scaling with the system size that is well described by the theoretical prediction for quantum chaotic systems. In the presence of measurements, we numerically find that the asymptotic SRE versus the coupling strength to the environment is well fitted by a generalized Lorentzian function. The scaling of the fitting parameters with the system size suggests that the asymptotic SRE linearly increases with the size in all the considered cases.

Entanglement is an important measure of quantum complexity and a relevant resource for quantum computation [1]. It is so crucial that it came as a surprise the recent discovery of a different yet independent measure of quantum complexity. This quantity is called non-stabilizerness (or "magic") and quantifies how much a pure state is far from the set of stabilizer states [2–12], which can be prepared applying Clifford quantum circuits. These circuits have the remarkable property of being efficiently classically simulatable despite being entangling [13]. Such a discovery has given rise to excitement in the scientific community, as witnessed by the flourishing amount of publications on this subject [2, 14–35].

Another research avenue dealing with quantum complexity that has emerged in recent times is the one of entanglement transitions in monitored systems. A monitored system is a quantum system that evolves under the effect of random measurements from an environment, that can be discrete as in the case of quantum circuits [13], or continuous as for quantum trajectories [36–38]. Quite importantly, for perfectly efficient measurements, the state along each trajectory is a pure one, and one gets the usual description in terms of density matrix evolving under a Lindblad equation only on average. On this pure state one can evaluate entanglement (usually by means of the half-system entanglement entropy) and study its behavior averaged over trajectories in the asymptotic regime.

It has been found that the interplay between the entangling effect of the unitary part of the dynamics and the disentangling effect of random measurements can give rise to different dynamical regimes where the entanglement entropy in the stationary regime scales differently with the system size. These entanglement transitions have been found in many contexts ranging from quantum circuits [39–59], to integrable or solvable [45, 60–87]

and nonintegrable [88–95] monitored Hamiltonian systems, and even in cases of measurement-only dynamics of nonlocal strings [96–98], and in the average density matrix of systems with power-law Lindbladians [99].

One could consider the behavior of the nonstabilizerness in monitored quantum systems as a different measure of quantum complexity. This analysis has been actually performed in the case of a Clifford quantum circuit to which random T gates creating magic and random projective measurements were applied, and a transition both in entanglement and magic was found [100]. In Ref. [101] it was argued that the entanglement transition occurs at a different point than the magic transition, so the question is still debated. Moreover, in a measurement-only circuit, a transition in the behavior of the magic has also been observed [102].

In this contribution we follow this line of research and consider two many-body quantum systems—namely, the staggered XXZ spin chain [103] and the Sachdev-Ye-Kitaev (SYK) model [104, 105]—in contact with an environment performing continuous measurements that, on average, provide a Lindblad evolution. We choose a specific homodyne measurement scheme, corresponding to the so-called quantum-state-diffusion unraveling. Averaging over the trajectories generated by this process gives rise to the Lindblad equation for observables. We consider the nonstabilizerness averaged over trajectories, for which the Lindblad approach cannot be applied due to the nonlinearity of this quantity in the quantum state.

To evaluate the nonstabilizerness, quantified through the stabilizer Rényi entropy (SRE) [22, 106], one must compute all expectations of the Pauli strings on the state, and we have found a way to make this more efficient compared to brute-force approaches. Efficient protocols based on Montecarlo sampling of the Pauli strings [107, 108] and others specifically tailored for

fermionic Gaussian states [109] already exist. In contrast, in our case we can sample all the Pauli strings, because we simplify the evaluation of the expectation of one of them. Our protocol is best suited for the case where the dynamics is restricted to a subspace. To be concrete, we consider a set of qubits and restrict to the subspace with a zero total magnetization along the z axis.

We consider the set $\mathcal{P}_L$ of the Pauli strings

$$\hat{P} = \prod_{j=1}^{L} \hat{\sigma}_j^{\alpha_j} , \tag{1}$$

with $\alpha_j = 0,\ 1,\ 2,\ 3$ ($\hat{\sigma}_j^0 \equiv \hat{\mathbb{I}}$, $\hat{\sigma}_j^1 \equiv \hat{\sigma}_j^x$, $\hat{\sigma}_j^2 \equiv \hat{\sigma}_j^y$, $\hat{\sigma}_j^3 \equiv \hat{\sigma}_j^z$, and $\hat{\sigma}_j^{(x,y,z)}$ are the usual spin-1/2 Pauli operators), and the state $|\psi_t\rangle$ of the system at time t. The SRE is defined as [22, 106]

$$\mathcal{M}_2(t) = -\ln\left[\frac{1}{4^L} \sum_{\hat{P} \in \mathcal{P}_L} \langle \psi_t | \hat{P} | \psi_t \rangle^4 \right]. \tag{2}$$

To evaluate the expectations $A_P = \langle \psi_t | \hat{P} | \psi_t \rangle$, we expand $|\psi_t\rangle$ on the basis of the simultaneous eigenstates of $\hat{\sigma}_j^z$ (the so-called computational basis):

$$|\psi_t\rangle = \sum_{\{s_j\}} C_{\{s_j\}} |\{s_j\}\rangle , \tag{3}$$

where we restrict to the $\mathcal{N}_L = \binom{L}{L/2}$ configurations $\{s_j\}$ such that $\sum_{j=1}^{L} s_j = 0$. We can write the Pauli expectation as $A_P = \sum_{\{s_j\},\{s'_j\}} C_{\{s_j\}}^* C_{\{s'_j\}} \langle \{s_j\} | \hat{P} | \{s'_j\} \rangle$. Because both the states $|\{s_j\}\rangle$ and the operators $\hat{P}$ have a product structure, we can write

$$\langle \{s_j\} | \hat{P} | \{s'_j\} \rangle = \prod_{j=1}^{L} \langle s_j | \hat{\sigma}_j^{\alpha_j} | s'_j \rangle . \tag{4}$$

The elements of this product can be easily evaluated as

$$\langle s_j | \hat{\sigma}_j^{\alpha_j} | s'_j \rangle = \delta_{\alpha_j,0}\, \delta_{s_j,s'_j} + \delta_{\alpha_j,1}(\delta_{s_j,s'_j+1} + \delta_{s_j,s'_j-1})$$
$$+ \delta_{\alpha_j,2}(-i\delta_{s_j,s'_j+1} + i\delta_{s_j,s'_j-1})$$
$$+ \delta_{\alpha_j,3}\, \delta_{s_j,s'_j}(\delta_{s_j,1} - \delta_{s_j,0}) . \tag{5}$$

Given a configuration $\{s_j\}$ and a Pauli operator $\hat{P}$, there exists one and only one configuration $\{s'_j\}$ such that $\langle s_j | \hat{\sigma}_j^{\alpha_j} | s'_j \rangle \neq 0$, which can be easily constructed as follows. Given a site j, if the operator $\hat{P}$ in Eq. (1) is such that $\alpha_j = 0$ or $\alpha_j = 3$, then $s'_j = s_j$, otherwise $s'_j = -s_j$. So the expectation of the Pauli operator $\hat{P}$ on the state $|\psi_t\rangle$ is given by

$$\langle \psi_t | \hat{P} | \psi_t \rangle = \sum_{\{s_j\}} \langle s_j | \hat{P} | s'_j \rangle\, C_{\{s_j\}}^* C_{\{s'_j\}} , \tag{6}$$

where the sum is restricted to the configurations $\{s_j\}$ such that $\sum_{j=1}^{L} s_j = \sum_{j=1}^{L} s'_j = 0$. The advantage with respect to the naive evaluation of the 4^L Pauli operators and their expectations on the state is that here we do not need to store them in the memory, and for each operator we have only one sum over $\mathcal{N}_L = \binom{L}{L/2}$ terms to perform, instead of evaluating the expectation of a $2^L \times 2^L$ matrix. In this way we can simulate up to $L = 14$ sites.

Let us now use this method to evaluate the SRE in the unitary dynamics of the following models.
(i) The XXZ spin chain in a staggered field [103]:

$$\hat{H}_{\text{XXZ}} = \sum_{j=1}^{L} \left[\frac{J}{2} \left(\hat{\sigma}_j^+ \hat{\sigma}_{j+1}^- + \text{h.c.} \right) + \frac{V}{4} \hat{\sigma}_j^z \hat{\sigma}_{j+1}^z + \frac{W}{2}(-1)^j \hat{\sigma}_j^z \right], \tag{7}$$

where $\hat{\sigma}_j^\pm = \left(\hat{\sigma}_j^x \pm i\hat{\sigma}_j^y \right)/2$ and we assume periodic boundary conditions ($\hat{\sigma}_L^\alpha \equiv \hat{\sigma}_1^\alpha$). In Eq. (7), the hopping term (J) is quadratic in the fermionic representation, the interaction term (V) is quartic, while the staggered field (W) breaks the Bethe-Ansatz integrability of the simple XXZ chain [110]. For $V = 0$, the above Hamiltonian is integrable as well, since it can be mapped onto a system of free fermions [111], through a Jordan-Wigner transformation [112].
(ii) The SYK model, in the spin language:

$$\hat{H}_{\text{SYK}} = \frac{1}{\sqrt{L^3}} \sum_{i,j,k,l=1}^{L} J_{ij,kl}\, \hat{\mathcal{S}}^i \hat{\sigma}_i^+ \hat{\mathcal{S}}^j \hat{\sigma}_j^+ \hat{\mathcal{S}}^k \hat{\sigma}_k^- \hat{\mathcal{S}}^l \hat{\sigma}_l^- , \tag{8}$$

where $\hat{\mathcal{S}}^j \equiv \prod_{\ell<j} \hat{\sigma}_\ell^z$ are the string operators. The couplings $J_{ij,kl}$ are independent Gaussian-distributed complex variables, with zero average $\langle\!\langle J_{ij,kl} \rangle\!\rangle = 0$ and variance $\langle\!\langle |J_{ij,kl}|^2 \rangle\!\rangle = J^2$, ($J \in \mathbb{R}$), satisfying $J_{ij,kl} = -J_{ji,kl} = -J_{ij,lk} = J_{kl,ij}^*$. The $L^{-3/2}$ prefactor in front of the interaction strength guarantees that the system bandwidth is of the order of L, for $L \to \infty$, so that extensivity of thermodynamic quantities as the energy is preserved. The SYK model in Eq. (8) is strongly quantum chaotic, being a fast scrambler of quantum information [113, 114], with all its eigenstates exhibiting volume-law entanglement entropy [115, 116].

For both Hamiltonians (7) and (8), we initialize the system in the factorized Néel state $|\uparrow,\downarrow,\uparrow,\downarrow,\ldots,\uparrow,\downarrow\rangle$ and perform the unitary dynamics using exact diagonalization or the Krylov technique as implemented in Expokit [117]. We also remark that both $\hat{H}_{\text{XXZ}}$ and $\hat{H}_{\text{SYK}}$ commute with the total magnetization operator $\hat{S}^z = \frac{1}{2} \sum_j \hat{\sigma}_j^z$, therefore our dynamics is restricted to the subspace with $\langle \psi_t | \hat{S}^z | \psi_t \rangle = 0$.

Some examples of the time evolution of the SRE (2) in the XXZ and SYK models are shown in Fig. 1 [panels (a) and (b), respectively]. We see that, in the SYK case, there are very small fluctuations around an average value, in stark contrast with the wide oscillations of the
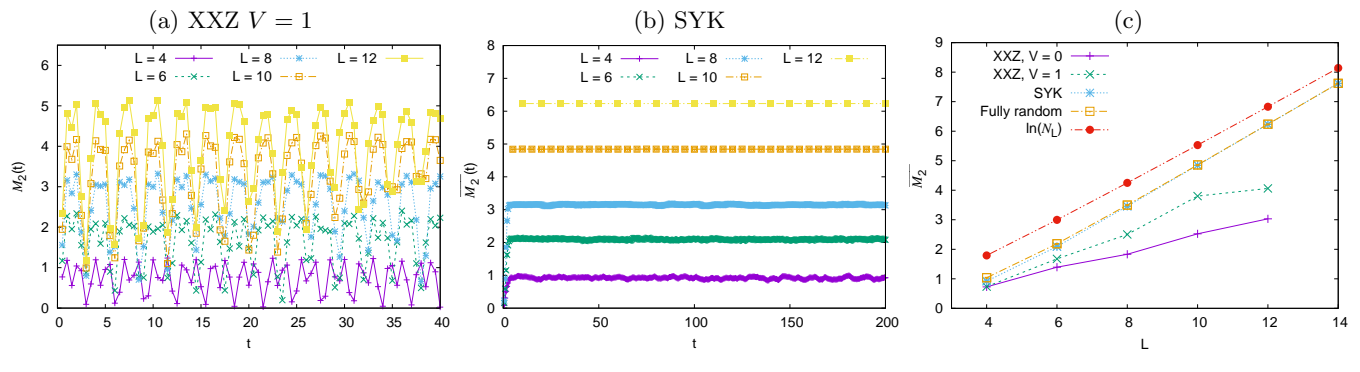
FIG. 1. (a) The SRE [$\mathcal{M}_2$ in Eq. (2)] vs time, for the unitary dynamics ($\gamma = 0$) induced by the staggered XXZ Hamiltonian (7) with $V = 1$ and $W = 1$. The various curves are for different system sizes (see legend). (b) Same as (a) but for the SYK model (8). In both panels, increasing values of SRE correspond to larger L. (c) The time-averaged SRE ($\overline{\mathcal{M}_2}$) vs L, for the staggered XXZ and the SYK model, compared with the corresponding result for the fully random state. For reference, we also plot the theoretically predicted [118] quantum-chaotic behavior $\overline{\mathcal{M}_2} \sim \ln(\mathcal{N}_L)$. Data in (b,c) for the SYK model and for the fully random case are averaged over $N_r = 48$ realizations. We set $J = 1$ in both models, thus fixing the energy scale. To simulate the real-time dynamics, we use exact diagonalization or Krylov technique with a time step $\delta t = 0.01$.

XXZ case. The SYK model is strongly quantum chaotic and displays a self-averaging behavior that erases fluctuations, also in the behavior of the SRE. Looking at the data in Fig. 1(c), which reports the time averages of the SRE as a function of the system size, we can observe that in all cases it grows approximately linearly with L. More specifically, it is larger in the interacting XXZ case ($V = 1$) rather than in the corresponding integrable tight-binding limit ($V = 0$), while it attains its maximum value for the SYK system. We then compare these curves with the SRE evaluated for a fully random state, given by $|\psi\rangle = \frac{1}{\sqrt{\mathcal{N}_L}} \sum_{\{s_j\}} e^{-i\varphi_{\{s_j\}}} |\{s_j\}\rangle$, where the sum is performed over the configurations such that $\sum_{j=1}^{L} s_j = 0$, and the $\varphi_{\{s_j\}}$ are random numbers uniformly distributed in $[0, 2\pi)$. Data are averaged over different realizations of the random state.

We see in Fig. 1(c) that the time average of the SRE for the SYK model saturates the bound provided by the fully random state, when $L \gtrsim 10$. Beyond that, both the average SRE of the SYK model and the one of the fully random state tend to be asymptotically parallel to the value $\ln \mathcal{N}_L$ given by the prediction of [118] for quantum chaotic systems. (We have checked that the ratio between the time-averaged magic of the SYK model and the theoretical quantum-chaotic prediction $\ln \mathcal{N}_L$ tends to 1 for increasing L.) It is interesting that this result is recovered at such small system sizes in the case of the SYK model, as it is the model displaying strongest quantum chaos.

Let us finally move to study the SRE in the monitored dynamics. We apply to both models a quantum-state-diffusion measurement protocol as in Ref. [65]. Here we choose to probe the onsite z magnetization operators $\hat{\sigma}_j^z$ as in Ref. [103]. Discretizing the time in steps δt and Trotterizing, we get the stochastic-Hamiltonian evolution

step, up to $o(\gamma \delta t)$ terms [65]

$$|\psi_{t+\delta t}\rangle = \mathcal{N} e^{\sum_l \hat{\sigma}_l^z [\delta \xi_l(t) + 2\gamma \delta t \langle \psi_t | \hat{\sigma}_l^z | \psi_t \rangle]} e^{-i\hat{H}\delta t} |\psi_t\rangle, \quad (9)$$

where γ is the coupling to the environment, $\delta \xi_l(t)$ are uncorrelated random Gaussian variables with vanishing average and variance $\gamma \delta t$, and $\mathcal{N}$ is a normalization factor. In writing this formula we could apply some simplifications due to the fact that the unitary plus noisy dynamics of both models conserves the total z magnetization, and we restrict to the subspace with $\langle \psi_t | \hat{S}^z | \psi_t \rangle = 0$, whose dimension is $\mathcal{N}_L = \binom{L}{L/2}$.

Each realization of the stochastic evolution provides a single quantum trajectory, along which we evaluate the SRE, $\mathcal{M}_2(t)$, as in Eq. (2). We mark with $\overline{\mathcal{M}_2}(t)$ the average of the SRE over N_r quantum trajectories at time t. Then we average over time, between an initial and a final value chosen such that stationarity has been attained. The SRE averaged over realizations and time is denoted by $\overline{\mathcal{M}_2}$. Each errorbar is computed as the root mean square deviation divided by the square root of the number of realizations $\sqrt{N_r}$. We still initialize the dynamics in the Néel state $|\uparrow, \downarrow, \uparrow, \downarrow, \ldots, \uparrow, \downarrow\rangle$ and use the same numerical techniques adopted to study the unitary dynamics. We remark that, for the XXZ model with $V = 0$, also the monitored dynamics is integrable [65].

Our numerical results for $\overline{\mathcal{M}_2}$ versus γ are reported in Fig. 2. Panel (a) is for the staggered XXZ model in the integrable tight-binding case [Eq. (7) with $V = 0$]. We see that, for each vale of L, the curve lies much below the value corresponding to the fully random state (horizontal dashed line with the same color code). On the other hand, the curves reported in Fig. 2(b) for the nonintegrable staggered XXZ model, Eq. (7) with $V = 1$, tend to the corresponding random-state value for $\gamma \to 0$. The same occurs for the SYK model of Eq. (8), where

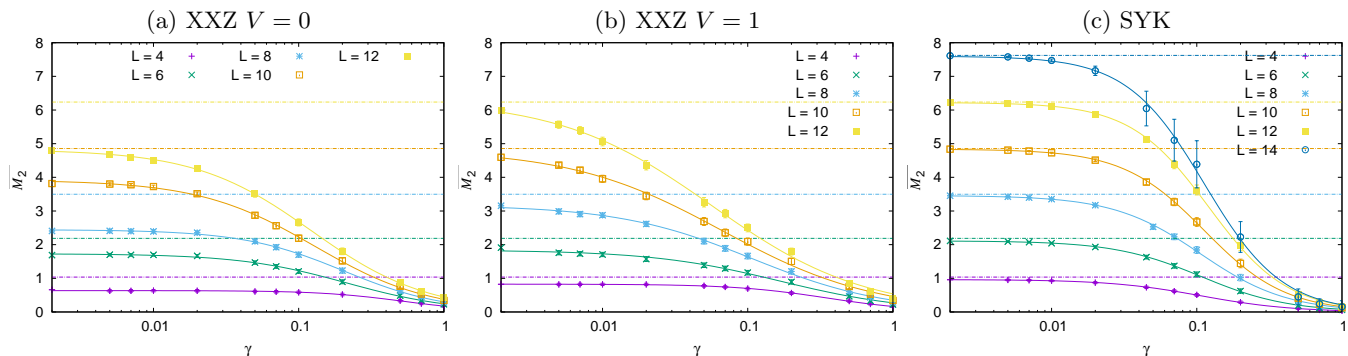FIG. 2. The SRE averaged over time and trajectories $\overline{\mathcal{M}_2}$, versus the coupling with the environment γ, in the monitored dynamics for the staggered spin-chain model of Eq. (7) with $W = 1$ and (a) $V = 0$, (b) $V = 1$, as well as for (c) the SYK model of Eq. (8). The various data sets are for different values of L (see legend). In all panels, increasing values of SRE correspond to larger L. Horizontal dashed lines indicate the fully-random-state value for the corresponding L. The fits to the numerical data (symbols), obtained with the least-square method applied to the function Eq. (10), are reported with continuous lines. The color code for the various quantities follows the corresponding values of L. We fix the energy scale by setting $J = 1$ in all models. Data for $L \leq 12$ are averaged over $N_{\mathrm{r}} = 48$ trajectories, while for $L = 14$ (only in the SYK model) we consider a single time and average over $N_{\mathrm{r}} \geq 11$ realizations, and get meaningful results due to the self-averaging property of the model.

convergence is attained for a larger value of γ, [Fig. 2(c)].

We observe an important difference between these latter two cases: while, in the SYK model, the $\gamma \to 0$ limit coincides with the average SRE in the unitary case shown in Fig. 1(c), in the staggered XXZ chain it does not, as only the limit $\gamma \to 0$ of the asymptotic SRE coincides with the result for the fully random state, while the average in the unitary case does not. This is a finite-size effect, due to the discreteness of the spectrum that affects the unitary dynamics of the XXZ model, and tends to disappear in the large-L limit or when a slight noise is applied. In the SYK case, these finite-size effects are much smaller [compare Fig. 1(a) with Fig. 1(b)], and a sort of self-averaging occurs that makes fluctuations around the average negligible, consistently with the fast-scrambler nature of the model.

In all the considered cases, we can fit the curves of $\overline{\mathcal{M}_2}$ versus γ with the generalized Lorentzian function

$$f_L(\gamma) = \frac{A_L}{1 + (\gamma/\gamma_{0,L})^{b_L}} \, . \tag{10}$$

(It reduces to the usual Lorentian for $b_L = 2$.) In fact, the result of this procedure is reported in the various panels of Fig. 2 by the continuous curves, which reliably fit all the symbols denoting numerical points. We do not understand the physical reason behind the fitting function reproducing the numerical points so well, and this will be the focus of further studies.

The values of the fitting parameters A_L, b_L, and $\gamma_{0,L}$ versus the size L are reported in Fig. 3. We see that A_L is linear in L and, for the nonintegrable cases, closely follows the fully-random-state value of the magic [Fig. 3(a)]. This is meaningful because A_L is the limit for $\gamma \to 0$ of $\overline{\mathcal{M}_2}$. We see moreover that the behaviors of b_L [Fig. 3(b)]

and of $\gamma_{0,L}$ [Fig. 3(c)] are compatible with an asymptotic convergence to a finite value, for increasing L. So our data suggest that in all the considered models the asymptotic SRE tends to a linear increase with the system size [embodied by A_L in Eq. (10)], whatever the value of the coupling with the environment. For large γ, the SRE tends anyway to 0, and the quantum-trajectory ensemble is drained of any quantum complexity. We notice also that the fluctuations around the average are maximum for $\gamma \sim 0.1$ and decrease moving towards the unitary ($\gamma \to 0$) or the factorized ($\gamma \to \infty$) limit.

In conclusion we have considered a monitored dynamics of many-body quantum systems undergoing continuous measurements, under the quantum-state-diffusion unraveling. We have focused on two Hamiltonians, the XXZ spin chain in a staggered field and the SYK model, where the former can be made interacting or integrable by changing a single parameter [either V or W in Eq. (7)], and the latter in Eq. (8) describes the most chaotic quantum system. We have evaluated the SRE along each quantum trajectory, as a probe of quantum-complexity properties different than entanglement.

To evaluate the SRE of Eq. (2), we have suggested a numerical procedure that takes advantage of the dynamics being restricted to a subspace and exploits the expansion of the state in the computational basis of classical spin configurations. The SRE is an average over expectations of Pauli operators, and we make the evaluation of these expectations more efficient. From one side we exploit that the matrix elements of Pauli operators between spin configurations are simple to evaluate. From the other we use that, given a spin configuration and a Pauli operator, there exists one and a single one configuration such that the matrix element is nonvanishing. In
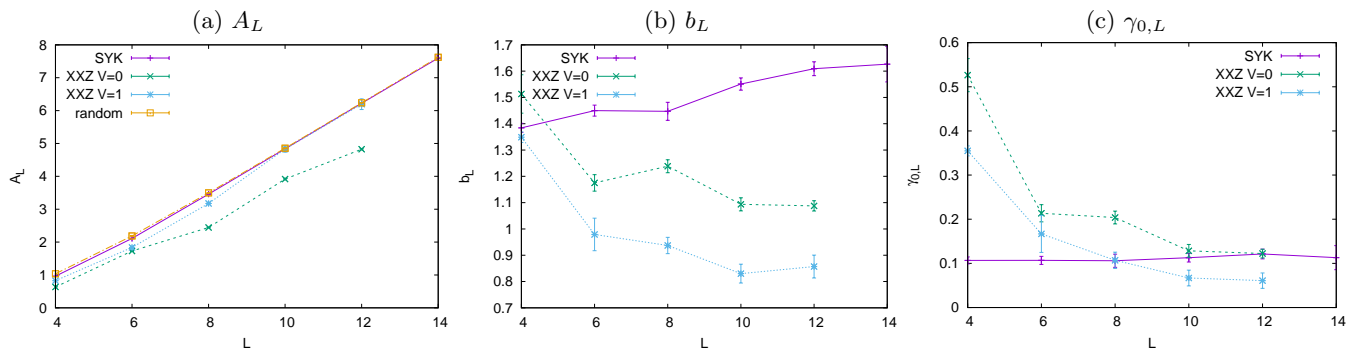
FIG. 3. Parameters of the fit with Eq. (10), for the averaged SRE $\overline{\mathcal{M}_2}$ vs γ, plotted against L. Specifically we plot (a) A_L, (b) b_L, and (c) $\gamma_{0,L}$. The various curves are for different models, as indicated in the legend. In panel (a) we also plot, for comparison, the fully-random-state value of the magic. Notice the linear increase in (a) and the saturation towards an asymptotic value in (b) and (c).

this way we can avoid to use memory resources to store the Pauli operators, and for each Pauli operator one can restrict to a single sum over the configurations in a restricted subspace, rather than evaluate the expectation over a state in the full Hilbert space.

Using this method we have first evaluated the SRE in the case of a pure unitary evolution. We have found that only in the SYK model—that is a fast scrambler and a strongly chaotic quantum system—the SRE after a transient attains an asymptotic value, and fluctuations in time around this value are negligible. Considering the time average, we see that in all models there is a behavior consistent with a linear increase in the system size. Only the SYK model saturates the bound provided by the fully random state when $L \geq 8$, and the SRE in this case tends to become asymptotically parallel to the logarithm of the Hilbert space dimension, as predicted for chaotic systems [118].

Then we have moved to the monitored case. Here the SRE averaged over quantum trajectories reaches an asymptotic value after a transient time. For both models, we have studied this asymptotic value for different system sizes and found that its dependence on the coupling to the measuring environment can be effectively fitted by a generalized Lorentzian function. From the scaling with the systems size of the fitting parameters we conclude that the asymptotic SRE is always linear in the system size, suggesting that any approximation of the state evolving under measurement with a stabilizer state becomes worse as the size increases.

Perspectives of future research include applying the methods of Ref. [109], dealing with an efficient evaluation procedure for the SRE in systems of noninteracting fermions, to describe the case of the noninteracting staggered spin-chain model for larger system sizes. Beyond that, one could apply to the nonintegrable cases the sampling scheme based on matrix product states described in Ref. [107]. Finally it would be interesting to

consider other monitored quantum systems, with the ultimate purpose to find a measurement transition in the behavior of the asymptotic SRE akin to the entanglement transitions.

[1] M. A. Nielsen and I. L. Chuang, *Quantum Computation and Quantum Information: 10th Anniversary Edition* (Cambridge University Press, Cambridge, UK, 2011).

[2] V. Veitch, S. A. H. Mousavian, D. Gottesman, and J. Emerson, The resource theory of stabilizer quantum computation, New J. Phys. **16**, 013009 (2014).

[3] M. Howard and E. Campbell, Application of a resource theory for magic states to fault-tolerant quantum computing, Phys. Rev. Lett. **118**, 090501 (2017).

[4] S. Bravyi and D. Gosset, Improved classical simulation of quantum circuits dominated by clifford gates, Phys. Rev. Lett. **116**, 250501 (2016).

[5] S. Bravyi, G. Smith, and J. A. Smolin, Trading classical and quantum computational resources, Phys. Rev. X **6**, 021043 (2016).

[6] S. Bravyi, D. Browne, P. Calpin, E. Campbell, D. Gosset, and M. Howard, Simulation of quantum circuits by low-rank stabilizer decompositions, Quantum **3**, 181

(2019).

[7] M. Heinrich and D. Gross, Robustness of Magic and Symmetries of the Stabiliser Polytope, Quantum **3**, 132 (2019).

[8] X. Wang, M. M. Wilde, and Y. Su, Quantifying the magic of quantum channels, New Journal of Physics **21**, 103002 (2019).

[9] X. Wang, M. M. Wilde, and Y. Su, Efficiently computable bounds for magic state distillation, Phys. Rev. Lett. **124**, 090505 (2020).

[10] A. Heimendahl, F. Montealegre-Mora, F. Vallentin, and D. Gross, Stabilizer extent is not multiplicative, Quantum **5**, 400 (2021).

[11] J. Jiang and X. Wang, Lower bound for the t count via unitary stabilizer nullity, Phys. Rev. Appl. **19**, 034052 (2023).

[12] T. Haug and M. Kim, Scalable measures of magic resource for quantum computers, PRX Quantum **4**, 010301 (2023).

[13] M. P. Fisher, V. Khemani, A. Nahum, and S. Vijay, Random quantum circuits, Annual Review of Condensed Matter Physics **14**, 335–379 (2023).

[14] D. Gottesman, Theory of fault-tolerant quantum computation, Phys. Rev. A **57**, 127 (1998).

[15] D. Gottesman, The Heisenberg representation of quantum computers, in *22nd International Colloquium on Group Theoretical Methods in Physics* (1998) pp. 32–43, arXiv:quant-ph/9807006.

[16] S. Bravyi, Lagrangian representation for fermionic linear optics, Quantum Inf. Comput. **5**, 216 (2005).

[17] M. Howard, J. Wallman, V. Veitch, and J. Emerson, Contextuality supplies the 'magic' for quantum computation, Nature **510**, 351 (2014).

[18] E. Chitambar and G. Gour, Quantum resource theories, Rev. Mod. Phys. **91**, 025001 (2019).

[19] J. R. Seddon and E. T. Campbell, Quantifying magic for multi-qubit operations, Proc. Roy. Soc. A (London) **475**, 20190251 (2019).

[20] S. Zhou, Z.-C. Yang, A. Hamma, and C. Chamon, Single T gate in a Clifford circuit drives transition to universal entanglement spectrum statistics, SciPost Phys. **9**, 087 (2020).

[21] Z.-W. Liu and A. Winter, Many-body quantum magic, PRX Quantum **3**, 020333 (2022).

[22] S. F. E. Oliviero, L. Leone, and A. Hamma, Magic-state resource theory for the ground state of the transverse-field ising model, Phys. Rev. A **106**, 042426 (2022).

[23] L. Leone, S. F. E. Oliviero, and A. Hamma, Nonstabilizerness determining the hardness of direct fidelity estimation, Phys. Rev. A **107**, 022429 (2023).

[24] D. Rattacaso, L. Leone, S. F. E. Oliviero, and A. Hamma, Stabilizer entropy dynamics after a quantum quench, Phys. Rev. A **108**, 042407 (2023).

[25] J. Odavić, T. Haug, G. Torre, A. Hamma, F. Franchini, and S. M. Giampaolo, Complexity of frustration: A new source of non-local non-stabilizerness, SciPost Phys. **4**, 131 (2023).

[26] L. Leone, S. F. E. Oliviero, G. Esposito, and A. Hamma, Phase transition in stabilizer entropy and efficient purity estimation, Phys. Rev. A **109**, 032403 (2024).

[27] E. Tirrito, P. S. Tarabunga, G. Lami, T. Chanda, L. Leone, S. F. E. Oliviero, M. Dalmonte, M. Collura, and A. Hamma, Quantifying nonstabilizerness through entanglement spectrum flatness, Phys. Rev. A **109**, L040401 (2024).

[28] A. Paviglianiti, G. Lami, M. Collura, and A. Silva, Estimating non-stabilizerness dynamics without simulating it (2024), arXiv:2405.06054 [quant-ph].

[29] N. Dowling, P. Kos, and X. Turkeshi, Magic of the heisenberg picture (2024), arXiv:2408.16047 [quant-ph].

[30] X. Turkeshi, A. Dymarsky, and P. Sierant, Pauli spectrum and magic of typical quantum many-body states (2023), arXiv:2312.11631 [quant-ph].

[31] X. Turkeshi, E. Tirrito, and P. Sierant, Magic spreading in random quantum circuits (2024), arXiv:2407.03929 [quant-ph].

[32] G. Passarelli, R. Fazio, and P. Lucignano, Nonstabilizerness of permutationally invariant systems, Phys. Rev. A **110**, 022436 (2024).

[33] G. Passarelli, P. Lucignano, D. Rossini, and A. Russomanno, Chaos and magic in the dissipative quantum kicked top (2024), arXiv:2406.16585 [quant-ph].

[34] P. Niroula, C. D. White, Q. Wang, S. Johri, D. Zhu, C. Monroe, C. Noel, and M. J. Gullans, Phase transition in magic with random quantum circuits (2024), arXiv:2304.10481 [quant-ph].

[35] M. Frau, P. S. Tarabunga, M. Collura, M. Dalmonte, and E. Tirrito, Nonstabilizerness versus entanglement in matrix product states, Phys. Rev. B **110**, 045101 (2024).

[36] M. B. Plenio and P. L. Knight, The quantum-jump approach to dissipative dynamics in quantum optics, Rev. Mod. Phys. **70**, 101 (1998).

[37] R. Fazio, J. Keeling, L. Mazza, and M. Schirò, Many-body open quantum systems (2024), arXiv:2409.10300 [quant-ph].

[38] A. J. Daley, Quantum trajectories and open many-body quantum systems, Adv. Phys. **63**, 77 (2014).

[39] Y. Li, X. Chen, and M. P. A. Fisher, Quantum Zeno effect and the many-body entanglement transition, Phys. Rev. B **98**, 205136 (2018).

[40] A. Chan, R. M. Nandkishore, M. Pretko, and G. Smith, Unitary-projective entanglement dynamics, Phys. Rev. B **99**, 224307 (2019).

[41] B. Skinner, J. Ruhman, and A. Nahum, Measurement-induced phase transitions in the dynamics of entanglement, Phys. Rev. X **9**, 031009 (2019).

[42] M. Szyniszewski, A. Romito, and H. Schomerus, Entanglement transition from variable-strength weak measurements, Phys. Rev. B **100**, 064204 (2019).

[43] A. C. Potter and R. Vasseur, Entanglement dynamics in hybrid quantum circuits, in *Quantum Science and Technology* (Springer International Publishing, Cham, 2022) pp. 211–249.

[44] Y. Bao, S. Choi, and E. Altman, Symmetry enriched phases of quantum circuits, Ann. Phys. **435**, 168618 (2021).

[45] A. Nahum and B. Skinner, Entanglement and dynamics of diffusion-annihilation processes with Majorana defects, Phys. Rev. Res. **2**, 023288 (2020).

[46] X. Chen, Y. Li, M. P. A. Fisher, and A. Lucas, Emergent conformal symmetry in nonunitary random dynamics of free fermions, Phys. Rev. Res. **2**, 033017 (2020).

[47] Y. Li, X. Chen, and M. P. A. Fisher, Measurement-driven entanglement transition in hybrid quantum circuits, Phys. Rev. B **100**, 134306 (2019).

[48] C.-M. Jian, Y.-Z. You, R. Vasseur, and A. W. W. Ludwig, Measurement-induced criticality in random quantum circuits, Phys. Rev. B **101**, 104302 (2020).

[49] Y. Li, R. Vasseur, M. P. A. Fisher, and A. W. W. Ludwig, Statistical mechanics model for Clifford random tensor networks and monitored quantum circuits, Phys. Rev. B **109**, 174307 (2024).

[50] M. Szyniszewski, A. Romito, and H. Schomerus, Universality of entanglement transitions from stroboscopic to continuous measurements, Phys. Rev. Lett. **125**, 210602 (2020).

[51] X. Turkeshi, R. Fazio, and M. Dalmonte, Measurement-induced criticality in $(2+1)$-dimensional hybrid quantum circuits, Phys. Rev. B **102**, 014315 (2020).

[52] O. Lunt, M. Szyniszewski, and A. Pal, Measurement-induced criticality and entanglement clusters: A study of one-dimensional and two-dimensional Clifford circuits, Phys. Rev. B **104**, 155111 (2021).

[53] P. Sierant, M. Schirò, M. Lewenstein, and X. Turkeshi, Measurement-induced phase transitions in $(d + 1)$-dimensional stabilizer circuits, Phys. Rev. B **106**, 214316 (2022).

[54] A. Nahum, S. Roy, B. Skinner, and J. Ruhman, Measurement and entanglement phase transitions in all-to-all quantum circuits, on quantum trees, and in Landau-Ginsburg theory, PRX Quantum **2**, 010352 (2021).

[55] A. Zabalo, M. J. Gullans, J. H. Wilson, S. Gopalakrishnan, D. A. Huse, and J. H. Pixley, Critical properties of the measurement-induced transition in random quantum circuits, Phys. Rev. B **101**, 060301 (2020).

[56] P. Sierant and X. Turkeshi, Universal behavior beyond multifractality of wave functions at measurement-induced phase transitions, Phys. Rev. Lett. **128**, 130605 (2022).

[57] G. Chiriacò, M. Tsitsishvili, D. Poletti, R. Fazio, and M. Dalmonte, Diagrammatic method for many-body non-Markovian dynamics: Memory effects and entanglement transitions, Phys. Rev. B **108**, 075151 (2023).

[58] K. Klocke and M. Buchhold, Majorana loop models for measurement-only quantum circuits, Phys. Rev. X **13**, 041028 (2023).

[59] A. Lira-Solanilla, X. Turkeshi, and S. Pappalardi, Multipartite entanglement structure of monitored quantum circuits (2024), arXiv:2412.16062 [quant-ph].

[60] M. Fava, L. Piroli, D. Bernard, and A. Nahum, Monitored fermions with conserved $u(1)$ charge, Phys. Rev. Res. **6**, 043246 (2024).

[61] K. Chahine and M. Buchhold, Entanglement phases, localization, and multifractality of monitored free fermions in two dimensions, Phys. Rev. B **110**, 054313 (2024).

[62] A. Delmonte, Z. Li, G. Passarelli, E. Y. Song, D. Barberena, A. M. Rey, and R. Fazio, Measurement-induced phase transitions in monitored infinite-range interacting systems (2024), arXiv:2410.05394 [quant-ph].

[63] D. Karevski, M. Coppola, E. Tirrito, and M. Collura, Measurments-induced quantum phase transitions (2024), arXiv:2412.06440 [cond-mat.stat-mech].

[64] G. Passarelli, X. Turkeshi, A. Russomanno, P. Lucignano, M. Schirò, and R. Fazio, Many-body dynamics in monitored atomic gases without postselection barrier, Physical Review Letters **132**, 10.1103/physrevlett.132.163401 (2024).

[65] X. Cao, A. Tilloy, and A. De Luca, Entanglement in a fermion chain under continuous monitoring, SciPost Phys. **7**, 24 (2019).

[66] M. Buchhold, Y. Minoguchi, A. Altland, and S. Diehl, Effective theory for the measurement-induced phase transition of Dirac fermions, Phys. Rev. X **11**, 041004 (2021).

[67] C.-M. Jian, B. Bauer, A. Keselman, and A. W. W. Ludwig, Criticality and entanglement in nonunitary quantum circuits and tensor networks of noninteracting fermions, Phys. Rev. B **106**, 134206 (2022).

[68] M. Coppola, E. Tirrito, D. Karevski, and M. Collura, Growth of entanglement entropy under local projective measurements, Phys. Rev. B **105**, 094303 (2022).

[69] M. Fava, L. Piroli, T. Swann, D. Bernard, and A. Nahum, Nonlinear sigma models for monitored dynamics of free fermions, Phys. Rev. X **13**, 041045 (2023).

[70] I. Poboiko, P. Pöpperl, I. V. Gornyi, and A. D. Mirlin, Theory of free fermions under random projective measurements, Phys. Rev. X **13**, 041046 (2023).

[71] C.-M. Jian, H. Shapourian, B. Bauer, and A. W. W. Ludwig, Measurement-induced entanglement transitions in quantum circuits of non-interacting fermions: Born-rule versus forced measurements (2023), preprint at: https://arxiv.org/abs/2302.09094, arXiv:2302.09094.

[72] J. Merritt and L. Fidkowski, Entanglement transitions with free fermions, Phys. Rev. B **107**, 064303 (2023).

[73] O. Alberton, M. Buchhold, and S. Diehl, Entanglement transition in a monitored free-fermion chain: From extended criticality to area law, Phys. Rev. Lett. **126**, 170602 (2021).

[74] X. Turkeshi, A. Biella, R. Fazio, M. Dalmonte, and M. Schirò, Measurement-induced entanglement transitions in the quantum ising chain: From infinite to zero clicks, Phys. Rev. B **103**, 224210 (2021).

[75] M. Szyniszewski, O. Lunt, and A. Pal, Disordered monitored free fermions, Phys. Rev. B **108**, 165126 (2023).

[76] X. Turkeshi, M. Dalmonte, R. Fazio, and M. Schirò, Entanglement transitions from stochastic resetting of non-hermitian quasiparticles, Phys. Rev. B **105**, L241114 (2021).

[77] G. Piccitto, A. Russomanno, and D. Rossini, Entanglement transitions in the quantum Ising chain: A comparison between different unravelings of the same Lindbladian, Phys. Rev. B **105**, 064305 (2022).

[78] G. Piccitto, A. Russomanno, and D. Rossini, Erratum: Entanglement transitions in the quantum Ising chain: A comparison between different unravelings of the same Lindbladian, Phys. Rev. B **106**, 219901(E) (2022).

[79] E. Tirrito, A. Santini, R. Fazio, and M. Collura, Full counting statistics as probe of measurement-induced transitions in the quantum Ising chain, SciPost Phys. **15**, 096 (2023).

[80] A. Paviglianiti and A. Silva, Multipartite entanglement in the measurement-induced phase transition of the quantum ising chain, Phys. Rev. B **108**, 184302 (2023).

[81] N. Lang and H. P. Büchler, Entanglement transition in the projective transverse field Ising model, Phys. Rev. B **102**, 094204 (2020).

[82] T. Minato, K. Sugimoto, T. Kuwahara, and K. Saito, Fate of measurement-induced phase transition in long-range interactions, Phys. Rev. Lett. **128**, 010603 (2022).

[83] C. Zerba and A. Silva, Measurement phase transitions in the no-click limit as quantum phase transitions of a non-hermitean vacuum, SciPost Phys. Core **6**, 051 (2023).

[84] A. Paviglianiti, X. Turkeshi, M. Schirò, and A. Silva, Enhanced entanglement in the measurement-altered

quantum ising chain (2023), preprint at: https://arxiv.org/abs/2310.02686, arXiv:2310.02686 [quant-ph].

[85] P. Chatterjee and R. Modak, Measurement-induced phase transition in periodically driven free-fermionic systems (2024), arXiv:2412.01917 [cond-mat.stat-mech].

[86] G. Piccitto, D. Rossini, and A. Russomanno, The impact of different unravelings in a monitored system of free fermions, Eur. Phys. J. B **97**, 90 (2024).

[87] Y. Le Gal, X. Turkeshi, and M. Schirò, Entanglement dynamics in monitored systems and the role of quantum jumps, PRX Quantum **5**, 10.1103/prxquantum.5.030329 (2024).

[88] O. Lunt and A. Pal, Measurement-induced entanglement transitions in many-body localized systems, Phys. Rev. Res. **2**, 043072 (2020).

[89] D. Rossini and E. Vicari, Measurement-induced dynamics of many-body systems at quantum criticality, Phys. Rev. B **102**, 035119 (2020).

[90] Q. Tang and W. Zhu, Measurement-induced phase transition: A case study in the nonintegrable model by density-matrix renormalization group calculations, Phys. Rev. Res. **2**, 013022 (2020).

[91] Y. Fuji and Y. Ashida, Measurement-induced quantum criticality under continuous monitoring, Phys. Rev. B **102**, 054302 (2020).

[92] P. Sierant, G. Chiriacò, F. M. Surace, S. Sharma, X. Turkeshi, M. Dalmonte, R. Fazio, and G. Pagano, Dissipative Floquet dynamics: from steady state to measurement induced criticality in trapped-ion chains, Quantum **6**, 638 (2022).

[93] E. V. H. Doggen, Y. Gefen, I. V. Gornyi, A. D. Mirlin, and D. G. Polyakov, Generalized quantum measurements with matrix product states: Entanglement phase transition and clusterization, Phys. Rev. Res. **4**, 023146 (2022).

[94] A. Altland, M. Buchhold, S. Diehl, and T. Micklitz, Dynamics of measured many-body quantum chaotic systems, Phys. Rev. Res. **4**, L022066 (2022).

[95] Z. Li, A. Delmonte, X. Turkeshi, and R. Fazio, Monitored long-range interacting systems: spin-wave theory for quantum trajectories (2024), arXiv:2405.12124 [quant-ph].

[96] M. Ippoliti, M. J. Gullans, S. Gopalakrishnan, D. A. Huse, and V. Khemani, Entanglement phase transitions in measurement-only dynamics, Phys. Rev. X **11**, 011030 (2021).

[97] A. Sriram, T. Rakovszky, V. Khemani, and M. Ippoliti, Topology, criticality, and dynamically generated qubits in a stochastic measurement-only kitaev model, Phys. Rev. B **108**, 094304 (2023).

[98] G. Piccitto, A. Russomanno, and D. Rossini, Entanglement dynamics with string measurement operators, SciPost Phys. Core **6**, 078 (2023).

[99] A. C. C. de Albornoz, D. C. Rose, and A. Pal, Entanglement transition and heterogeneity in long-range quadratic lindbladians, Phys. Rev. B **109**, 214204 (2024).

[100] M. Bejan, C. McLauchlan, and B. Béri, Dynamical magic transitions in monitored clifford+t circuits, PRX Quantum **5**, 030332 (2024).

[101] G. E. Fux, E. Tirrito, M. Dalmonte, and R. Fazio, Entanglement – nonstabilizerness separation in hybrid quantum circuits, Phys. Rev. Res. **6**, L042030 (2024).

[102] P. S. Tarabunga and E. Tirrito, Magic transition in measurement-only circuits (2024), arXiv:2407.15939 [quant-ph].

[103] B. Xing, X. Turkeshi, M. Schiró, R. Fazio, and D. Poletti, Interactions and integrability in weakly monitored hamiltonian systems, Phys. Rev. B **109**, L060302 (2024).

[104] S. Sachdev and J. Ye, Gapless spin-fluid ground state in a random quantum heisenberg magnet, Phys. Rev. Lett. **70**, 3339 (1993).

[105] A. Y. Kitaev, Entanglement in strongly correlated quantum matter, in Proceedings of KITP, University of California, Santa Barbara (2015).

[106] L. Leone, S. F. E. Oliviero, and A. Hamma, Stabilizer rényi entropy, Phys. Rev. Lett. **128**, 050402 (2022).

[107] G. Lami and M. Collura, Quantum magic via perfect pauli sampling of matrix product states (2023), arXiv:2303.05536 [quant-ph].

[108] Y.-M. Ding, Z. Wang, and Z. Yan, Evaluating many-body stabilizer rényi entropy by sampling reduced pauli strings: singularities, volume law, and nonlocal magic (2025), arXiv:2501.12146 [quant-ph].

[109] M. Collura, J. D. Nardis, V. Alba, and G. Lami, The quantum magic of fermionic gaussian states (2024), arXiv:2412.05367 [quant-ph].

[110] F. Franchini, *An Introduction to Integrable Techniques for One-Dimensional Quantum Systems* (Springer International Publishing, 2017).

[111] G. B. Mbeng, A. Russomanno, and G. E. Santoro, The quantum Ising chain for beginners, SciPost Phys. Lect. Notes , 82 (2024).

[112] E. Lieb, T. Schultz, and D. Mattis, Two soluble models of an antiferromagnetic chain, Annals of Physics **16**, 407 (1961).

[113] J. Maldacena and D. Stanford, Remarks on the sachdev-ye-kitaev model, Phys. Rev. D **94**, 106002 (2016).

[114] D. A. Roberts, D. Stanford, and A. Streicher, Operator growth in the syk model, Journal of High Energy Physics **2018**, 10.1007/jhep06(2018)122 (2018).

[115] C. Liu, X. Chen, and L. Balents, Quantum entanglement of the Sachdev-Ye-Kitaev models, Phys. Rev. B **97**, 245126 (2018).

[116] Y. Huang and Y. Gu, Eigenstate entanglement in the sachdev-ye-kitaev model, Phys. Rev. D **100**, 041901 (2019).

[117] R. Sidje, Expokit: A software package for computing matrix exponentials, ACM Trans. Math. Softw. **24**, 130 (1998).

[118] L. Leone, S. F. E. Oliviero, Y. Zhou, and A. Hamma, Quantum Chaos is Quantum, Quantum **5**, 453 (2021).